

不同外加电位下 X80 管线钢 在近中性 pH 溶液环境中的裂纹扩展行为研究

李琼, 刘智勇, 杜翠薇, 李晓刚, 刘然克

(北京科技大学 腐蚀与防护中心, 北京 100083)

摘要: 目的 研究不同外加电位下, X80 管线钢在近中性 pH 溶液环境中的裂纹扩展行为。方法 对 X80 管线钢紧凑拉伸试样进行近中性 pH 溶液环境中的循环加载试验, 利用拍摄装置记录不同循环次数下的裂纹长度, 并利用扫描电镜(SEM)观察裂纹扩展面上的微观形貌。研究不同外加电位下, X80 钢在近中性 pH 溶液环境中的裂纹扩展速率, 分析其裂纹扩展规律。结果 在开路条件下, 循环加载 755 次时, 裂纹扩展 4.6 mm 后失稳断裂; 在外加电位为 -775 mV (vs. SCE) 的条件下, 循环加载 671 次时, 裂纹扩展 3.677 mm 后失稳断裂; 在外加电位为 -1125 mV (vs. SCE) 的条件下, 循环加载 625 次时, 裂纹扩展 3.882 mm 后失稳断裂。结论 在开路电位和弱阴极电位下, 裂纹扩展受到阳极溶解机制和氢脆机制的混合控制, 以阳极溶解机制为主, 裂纹扩展速率均较低; 随着外加电位降低, 裂纹扩展机制逐渐过渡为主要受氢致开裂作用控制, 裂纹扩展速率显著增加。

关键词: X80 管线钢; 外加电位; 近中性 pH; 裂纹扩展

中图分类号: TG172.4 文献标识码: A 文章编号: 1001-3660(2015)03-0031-05

DOI: 10.16490/j.cnki.issn.1001-3660.2015.03.005

Crack Propagation Behaviour of X80 Pipeline Steel in Near-neutral pH Solution under Different Applied Potential

LI Qiong, LIU Zhi-yong, DU Cui-wei, LI Xiao-gang, LIU Ran-ke

(Corrosion and Protection Center, University of Science and Technology Beijing, Beijing100083, China)

ABSTRACT: **Objective** To study the crack propagation behavior of X80 pipeline steel in near-neutral pH solution under different applied potential. **Methods** The cyclic loading experiment of X80 pipeline steel compact tension (CT) specimen under different applied potential was conducted and the crack length was recorded by a magnifying glass during the experiment. After the cyclic loading experiment, the micro-morphology of crack propagation surface was observed by Scanning electron microscope (SEM). The crack propagation rate of X80 pipeline steel in near-neutral pH solution under different applied potential and the crack propagation

收稿日期: 2014-11-12; 修订日期: 2015-01-04

Received: 2014-11-12; Revised: 2015-01-04

基金项目: 国家高技术研究发展计划(863 计划, 2012AA040105); 国家自然科学基金(51471034); 北京市青年英才计划资助

Fund: Supported by the National High Tech R & D Program of China (2012AA040105), the National Nature Science Foundation of China (51471034) and Beijing Higher Education Young Elite Teacher Project

作者简介: 李琼(1990—), 女, 陕西人, 硕士, 主要研究管线钢应力腐蚀行为机理。

Biography: LI Qiong(1990—), Female, from Shaanxi, Master, Research focus: SCC mechanism of pipeline steels.

通讯作者: 刘智勇(1978—), 男, 吉林人, 博士, 副教授, 主要从事应力腐蚀方面的研究。

Corresponding author: LIU Zhi-yong(1978—), Male, from Jilin, Ph. D., Associate professor, Research focus: SCC of materials.

rule was analyzed. **Results** The brittle unstable fracture of CT specimen under open circuit condition occurred after 755 cycles and the crack propagation length was 4.6 mm. The brittle unstable fracture of CT specimen under an applied potential of -775 mV (vs. SCE) occurred after 671 cycles and the crack propagation length was 3.677 mm. The brittle unstable fracture of CT specimen under an applied potential of -1125 mV (vs. SCE) occurred after 625 cycles and the crack propagation length was 3.882 mm.

Conclusion The crack propagation of X80 pipeline steel in near-neutral pH solution under open circuit condition and weak cathode potential was mix-controlled by anodic dissolution mechanism and hydrogen embrittlement mechanism, dominated by the anodic dissolution mechanism, and the crack propagation rate was low. With the decrease of the applied potential, the crack propagation mechanism was gradually dominated by the hydrogen embrittlement mechanism, and the crack propagation rate was obviously increased.

KEY WORDS: X80 pipeline steel; applied potential; near-neutral pH; crack propagation behavior

埋地长输管道是目前长距离运输石油、天然气的主要方式,但是土壤介质诱发埋地管道发生应力腐蚀开裂(SCC),会严重威胁其安全运行^[1]。

管线钢 SCC 主要分为高 pH-SCC 和近中性 pH-SCC。高 pH-SCC 主要发生在 pH 值为 8~10.5 的环境中,与高浓度的碳酸盐和碳酸氢盐密切相关。碳酸盐和碳酸氢盐主要由土壤中的 CO_2 和阴极保护作用产生的 OH^- 经过一系列反应生成。高 pH-SCC 发生的电位区间为 $-550 \sim -650$ mV (如无特别说明,文中的电位均相对于 SCE),发生条件为:管道表面涂层剥离,导致阴极保护电流被部分屏蔽,阴极保护作用不足^[2-4]。其断口形貌表现为沿晶型开裂。目前普遍认为,高 pH-SCC 主要是由于钝化膜破裂,导致晶界处优先发生阳极溶解引起的^[5-6]。

近中性 pH-SCC 主要发生在 pH 值为 6~8 的环境中,与土壤中的碳酸氢盐密切相关^[7-8]。近中性 pH-SCC 发生条件为:管道表面涂层剥离,导致阴极保护电流被完全屏蔽,阴极保护作用完全失效。其断口形貌表现为穿晶型开裂^[9-11]。此外有研究表明,环境中的氢、 CO_2 及硫酸盐还原菌(SRB)对近中性 pH-SCC 具有重要影响^[12-14]。Liu^[15-17]研究了 X70 管线钢在阴极保护(CP)条件下,在近中性 pH 溶液中的 SCC 机理。结果表明,在阴极极化状态下,存在一临界电位范围($-730 \sim -920$ mV),在该电位范围内,管线钢裂纹尖端处于非稳态电化学状态,有发生阳极溶解(AD)的可能。当极化电位高于该临界范围时,SCC 为 AD 机制;当极化电位低于该临界范围时,SCC 为氢脆(HE)机制;当极化电位处于该临界范围内时,SCC 是 AD 和 HE 混合机制。不过,上述研究结果缺乏裂纹扩展试验和裂纹尖端电化学试验结果的印证。

文中进行了不同外加电位下,X80 管线钢在近中性 pH 溶液中的裂纹扩展行为实验研究,为进一步明确近中性 pH-SCC 过程中裂尖的扩展机制提供支持和依据。

1 试验

材料为宝钢产 X80 管线钢,金相组织形貌见图 1,主要由贝氏体及少量铁素体组成。其化学成分(以质量分数计)为:C 0.061%,Si 0.19%,Mn 1.75%,P 0.012%,S 0.001%,Cr 0.033%,Ni 0.21%,Cu 0.16%,Nb 0.045%,Fe 余量。其力学性能为:屈服强度 $\sigma_{0.2} = 540$ MPa,抗拉强度 $\sigma_b = 680$ MPa。

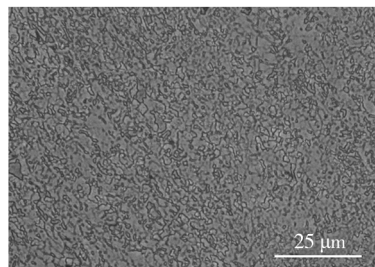


图 1 宝钢 X80 管线钢金相组织形貌

Fig. 1 Microstructure of the BAOSTEEL X80 pipeline steel

根据近中性 pH 溶液——NS4 溶液的化学组成配制模拟液: NaHCO_3 0.483 g/L, KCl 0.122 g/L, CaCl_2 0.137 g/L, $\text{MgSO}_4 \cdot 7\text{H}_2\text{O}$ 0.131 g/L。实验前,需向溶液中持续通入 5% CO_2 -95% N_2 (体积分数)混合气 24 h,以除去溶液中的氧气,同时使其 pH 维持在 6.6~6.8。在实验过程中仍需持续通入混合气,维持无氧状态和近中性 pH 环境。

采用 LETRY WDML-30kN 型微机控制慢应变速率拉伸试验机对紧凑拉伸(CT)试样进行循环加载试验。试验采用分级加载方式,最大应力为 17 500 N,最小应力设为 10 000 N,加载速率为 0.5 mm/min。CT 试样的尺寸见图 2,其厚度为 10 mm。首先在 CT 试样上预制 3 mm 左右的裂纹,分别用 60#, 240#, 400#, 800#, 1500# 砂纸逐级打磨两个表面,保证最后一道打磨方向垂直于裂纹扩展方向,以便准确测量预制裂纹的长度。预制裂纹结束后,在试样背面焊接铜导

线并用硅胶密封好,以便施加外加电位。然后用砂纸将试样正面逐级打磨至 2000#,并且保证打磨方向垂直于裂纹扩展方向。最后用丙酮和乙醇对试样进行清洁,包括试样表面和切口内位置,吹干备用。

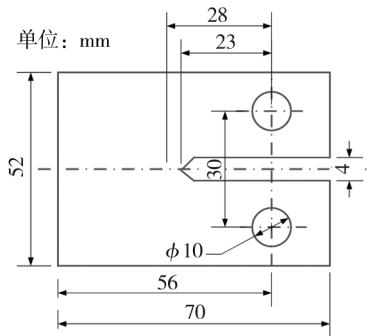


图 2 紧凑拉伸试样形状及尺寸

Fig. 2 Shape and dimension of compact tension (CT) specimen

利用恒电位仪对试样施加外加电位,分别进行开路条件(−730 ~ −750 mV)及−775, −1125 mV(相当于相对 Cu/CuSO₄ 电极的开路条件及−850, −1200 mV)三种条件下的裂纹扩展试验。使用长焦距放大镜记录循环加载不同次数后的裂纹长度和裂纹扩展形貌。

裂纹扩展试验结束后,对试样进行切割,得到裂纹扩展面。先用除锈液(500 mL 浓盐酸+500 mL 去离子水+10 g 六次甲基四胺)超声清洗 3 min,然后用酒精超声清洗,取出后吹干,最后用 FEI Quanta 250 型环境扫描电子显微镜(SEM)观察裂纹扩展面的微观形貌。

2 结果及分析

2.1 裂纹扩展行为

记录循环不同次数后的裂纹长度,可以得到三种条件下裂纹扩展长度随循环次数的变化规律,如图 3 所示。利用公式(1)可以将图 3 中的关系转换为裂纹扩展速率 da/dN 与应力强度因子幅值 ΔK 之间的关系,如图 4 所示。式(1)中: P_{max} 为最大应力 17 500 N, P_{min} 为最小应力 10 000 N, B 为试样厚度 10 mm, W 为 56 mm, a 为瞬时裂纹长度。

$$\Delta K = \frac{P_{\max} - P_{\min}}{BW^{1/2}} \frac{\left(2 + \frac{a}{W}\right) \left(\frac{a}{W}\right)^{1/2}}{\left(1 - \frac{a}{W}\right)^{3/2}} \left[0.886 + 4.64 \times \frac{a}{W} - 13.32 \times \left(\frac{a}{W}\right)^2 + 14.72 \times \left(\frac{a}{W}\right)^3 - 5.6 \times \left(\frac{a}{W}\right)^4 \right] \quad (1)$$

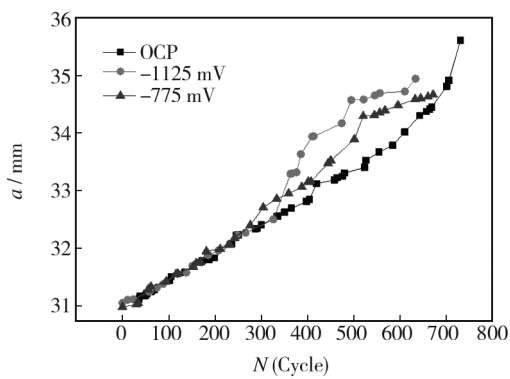


图 3 不同外加电位下裂纹扩展长度与循环次数的关系
Fig. 3 The relationship between the crack propagation length and cycle number of X80 pipeline steel in near-neutral pH solution under different applied potential

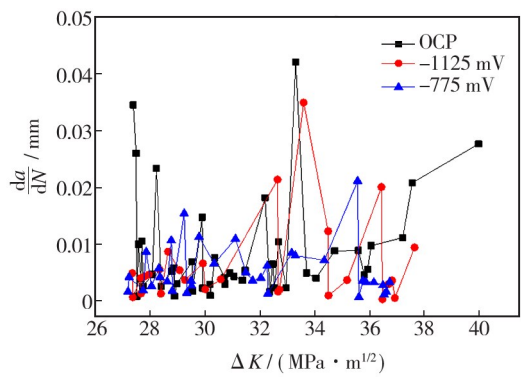


图 4 不同外加电位下裂纹扩展速率与应力强度、应力幅值的关系
Fig. 4 The relationship between the crack propagation rate and stress intensity factor range of X80 pipeline steel in near-neutral pH solution under different applied potential

在开路条件下,循环加载了 755 次后,裂纹扩展了 4.6 mm 发生失稳断裂;当外加电位为−775 mV 时,循环加载了 671 次后,裂纹扩展了 3.667 mm 发生失稳断裂;当外加电位为−1125 mV 时,循环加载了 671 次后,裂纹扩展了 3.882 mm 发生失稳断裂。由此得到不同外加电位下,X80 管线钢在近中性 pH 溶液环境中的平均裂纹扩展速率,如图 5 所示。

由于紧凑拉伸试样的初始裂纹长度并不一致,因此图 3 中只考虑某一循环次数时的裂纹长度是不科学的。从图 4 中可以发现,外加−1125 mV 和开路条件下,数据点大多在外加−775 mV 的上方,表明这两种条件下的裂纹扩展速率更大。这也与图 5 中不同外加电位下,X80 管线钢在近中性 pH 溶液环境中的平均裂纹扩展速率变化规律一致。由上述分析可知,在不同外加电位下,X80 管线钢在近中性 pH 溶液环

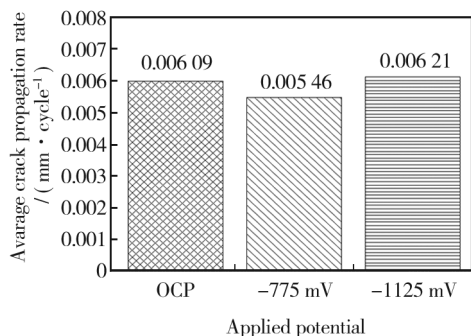


图 5 不同外加电位下平均裂纹扩展速率

Fig.5 The average crack propagation rate of X80 pipeline steel in near-neutral pH solution under different applied potential

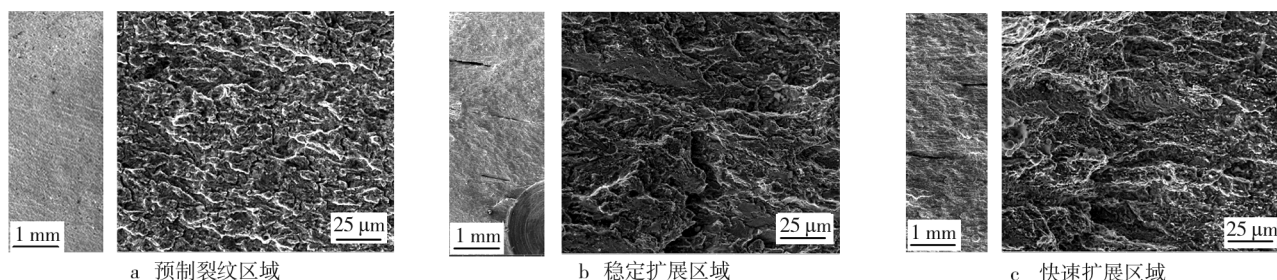
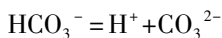
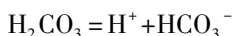


图 6 开路条件下的裂纹扩展面形貌

Fig.6 The morphology of crack propagation surface of X80 pipeline steel in near-neutral pH solution under the condition of open circuit: a) pre-fatigue cracking zone, b) stable propagation zone, c) unstable propagation zone

2.3 应力腐蚀过程分析

NS4 溶液中的反应有^[18]:



X80 管线钢在近中性 pH 溶液环境 (NS4 溶液) 中的电化学反应如下:

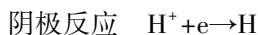
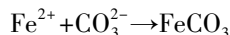
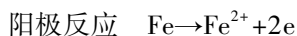


图 7 为 X80 管线钢在近中性 pH 溶液中的快、慢扫描极化曲线。根据快慢扫描极化曲线,可将电位范围分为 3 个部分,这 3 个部分也分别代表了 3 种不同的 SCC 机制^[19]:

1) 当电位高于 -740 mV 时,裂纹尖端和裂纹壁部位均呈阳极溶解特征,主要发生 Fe 的活性溶解。这表明在该电位范围内,SCC 行为受阳极溶解机制控制。

2) 当电位低于 -880 mV 时,阳极溶解过程被强烈抑制,裂纹尖端和裂纹壁部位均呈阴极过程特征,阴极析氢过程随着电位的降低而增强。这表明在该电位范围内,SCC 行为受氢致开裂机制控制。

境中的裂纹扩展速率存在差异,速率由大到小的外加电位条件为: -1125 mV > OCP > -775 mV。

2.2 断口形貌分析

图 6 为紧凑拉伸试样循环加载试验完成后,沿裂纹内扩展面分开的形貌。从图 6a 可以发现,预制裂纹区域在溶液中发生了局部腐蚀;从图 6b 可以发现,稳定扩展区域扩展面上有明显的脆性开裂特征;从图 6c 可以发现,裂纹快速扩展区域有明显的撕裂特征。并且,在稳定扩展区域和裂纹快速扩展区域均存在与裂纹扩展方向垂直的较宽长直裂纹。

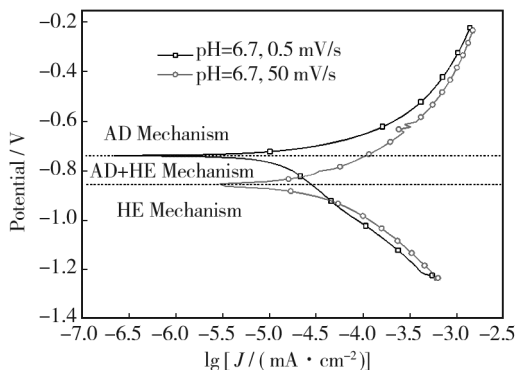


图 7 X80 管线钢在近中性 pH 溶液环境中的快慢扫描极化曲线
Fig.7 The fast and slow sweep curves of X80 pipeline steel in near-neutral pH solution

3) 当电位处于 -740 ~ -880 mV 时,裂纹尖端呈阳极溶解特征,而裂纹壁部位呈阴极析氢特征,并且可以发现随着电位的负移,裂纹尖端的阳极溶解过程逐渐被抑制,而裂纹壁上阴极析氢过程逐渐被促进。这表明在该电位范围内,SCC 行为受阳极溶解和氢致开裂机制混合控制。

结合图 3—5 中的裂纹扩展速率可以发现,与开路条件下 (-730 ~ -750 mV) 相比,当外加电位为

-775 mV时,裂纹扩展速率没有发生明显改变,只存在极不明显的降低;当外加电位负移至-1125 mV时,裂纹扩展速率明显增大。该现象与图7中X80管线钢在近中性pH溶液中的快慢扫描极化曲变化规律一致。分析原因如下:当电位从开路电位略微负移至-775 mV时,裂纹尖端的阳极溶解过程被部分抑制,同时由于电位负移对裂纹壁部位阴极析氢过程的促进作用并不明显,因此与开路条件下阳极溶解机制控制过程相比,裂纹扩展速率基本相当,只发生了略微降低;当外加电位负移至-1125 mV时,阳极反应受到强烈抑制,阴极电流密度大大增加,产生大量的氢,氢不断渗入钢中,逐渐成为裂纹扩展的主导因素,应力腐蚀敏感性大大提高,因此在该外加电位条件下的裂纹扩展最快^[20]。

从以上分析可以发现,外加电位对于X80管线钢在近中性pH溶液环境(NS4溶液)中的裂纹扩展行为具有显著影响。开路条件下(-730~-750 mV),裂纹扩展主要受阳极溶解机制控制;当施加外加电位时,裂纹扩展机制和裂纹扩展速率均发生变化。当外加电位(-775 mV)略低于开路电位时,裂纹扩展受阳极溶解和氢致开裂机制混合控制,并且阳极溶解过程随电位负移逐渐被抑制,阴极析氢过程随电位负移逐渐被加强,因而裂纹扩展速率略微降低。可以推断,随着外加电位进一步降低,阳极溶解过程的抑制作用和阴极析氢过程的促进作用均逐渐增强,裂纹扩展机制逐渐过渡为主要受氢致开裂作用控制。因此,当外加电位负移至某一电位时,裂纹扩展速率就会增大。当外加电位继续负移(低于-880 mV)时,裂纹扩展完全受氢致开裂机制控制,并且随着电位负移,阴极析氢过程的促进作用更为明显,裂纹扩展速率也大大增加。

3 结论

外加电位对于X80管线钢在近中性pH溶液环境(NS4溶液)中的裂纹扩展机制和裂纹扩展速率均具有显著影响。在开路电位和弱阴极电位下,裂纹扩展受到阳极溶解机制和氢脆机制的混合控制,以阳极溶解机制为主。当外加的阴极电位较弱时,由于阳极溶解过程被部分抑制,裂纹扩展速率仅比开路电位下略微降低。随着外加电位进一步降低,裂尖阳极溶解过程进一步受到抑制,阴极析氢过程逐渐增强,裂纹扩展机制逐渐过渡为主要受氢致开裂作用控制。当外加电位负移至-1125 mV时,裂纹扩展完全受氢致

开裂机制控制,并且随着电位负移,阴极析氢过程的促进作用更为明显,裂纹扩展速率也显著增加。

参考文献

- [1] COLE I S, MARNEY D. The Science of Pipe Corrosion: A Review of the Literature on the Corrosion of Ferrous Metals in Soils[J]. Corrosion Science, 2012, 56: 5—16.
- [2] SONG F M Predicting the Mechanisms and Crack Growth Rates of Pipelines Undergoing Stress Corrosion Cracking at High pH[J]. Corrosion Science, 2009, 51: 2657—2674.
- [3] OSKUIE A A, SHAHRABI T, SHAHRABI A, et al. Electrochemical Impedance Spectroscopy Analysis of X70 Pipeline Steel Stress Corrosion Cracking in High pH Carbonate Solution[J]. Corrosion Science, 2012, 61: 111—122.
- [4] PARKINS R N, O'DEL C S, FESSLER R R. Factors Affecting the Potential of Galvanostatically Polarised Pipeline Steel in Relation to SCC in CO_3^{2-} - HCO_3^- Solutions[J]. Corrosion Science, 1984, 24(4): 343—374.
- [5] WANG J Q, ATRENSA A. SCC Initiation for X65 Pipeline Steel in the "High" pH Carbonate/Bicarbonate Solution[J]. Corrosion Science, 2003, 45(10): 2199—2217.
- [6] MUSTAPHA, CHARLES E A, HARDIE D. Evaluation of Environment-assisted Cracking Susceptibility of a Grade X100 Pipeline Steel[J]. Corrosion Science, 2012, 54: 5—9.
- [7] JAVIDI M, HOREH S B. Investigating the Mechanism of Stress Corrosion Cracking in Near-neutral and High pH Environments for API 5L X52 Steel[J]. Corrosion Science, 2014, 80: 213—220.
- [8] LU B T, SONG F, GAO M, et al. Crack Growth Model for Pipelines Exposed to Concentrated Carbonate-Bicarbonate Solution with High pH[J]. Corrosion Science, 2010, 52: 4064—4072.
- [9] XU L Y, CHENG Y F. An Experimental Investigation of Corrosion of X100 Pipeline Steel under Uniaxial Elastic Stress in a Near-neutral pH Solution[J]. Corrosion Science, 2012, 59: 103—109.
- [10] XU L Y, CHENG Y F. Corrosion of X100 Pipeline Steel under Plastic Strain in a Neutral pH Bicarbonate Solution[J]. Corrosion Science, 2012, 64: 145—152.
- [11] LU B T, LUO J L, NORTON P R. Environmentally Assisted Cracking Mechanism of Pipeline Steel in Near-neutral pH Groundwater[J]. Corrosion Science, 2010, 52: 1787—1795.
- [12] XUE H B, CHENG Y F. Photo-electrochemical Studies of the Local Dissolution of a Hydrogen-charged X80 Steel at Crack-tip in a Near-neutral pH Solution[J]. Electrochimica Acta, 2010, 55(20): 5670—5676.

- of Metallic Zinc Dust in Heavy Duty Protective Coatings by Conducting Polymer [J]. *Progress in Organic Coatings*, 2010, 69:26—30.
- [4] NG C B, SCHADLER L S, SIEGEL R W. Synthesis and Mechanical Properties of TiO_2 -epoxy Nanocomposites [J]. *Nanostructured Materials*, 1999 (12): 507—510.
- [5] SHI H, LIU F, YANG L, et al. Characterization of Protective Performance of Epoxy Reinforced with Nanometer-sized TiO_2 and SiO_2 [J]. *Progress in Organic Coatings*, 2008, 62: 359—368.
- [6] LEWIS O D, CRITCHLOW G W, WILCOX G D, et al. A Study of the Corrosion Resistance of a Waterborne Acrylic Coating Modified with Nano-sized Titanium Dioxide [J]. *Progress in Organic Coatings*, 2012, 73: 88—94.
- [7] DHOKE S K, KHANNA A. Electrochemical Impedance Spectroscopy (EIS) Study of Nano-alumina Modified Alkyd Based Waterborne Coatings [J]. *Progress in Organic Coatings*, 2012, 74: 92—99.
- [8] RASHVAND M, RANJBAR Z. Effect of Nano-ZnO Particles on the Corrosion Resistance of Polyurethane-based Waterborne Coatings Immersed in Sodium Chloride Solution Via EIS Technique [J]. *Progress in Organic Coatings*, 2013, 76: 1413—1417.
- [9] LEWIS O, CRITCHLOW G, WILCOX G, et al. A Study of the Corrosion Resistance of a Waterborne Acrylic Coating Modified with Nano-sized Titanium Dioxide [J]. *Progress in Organic Coatings*, 2012, 73: 88—94.
- [10] CALVERT P. Nanotube Composites: A Recipe for Strength [J]. *Nature*, 1999, 399: 210—211.
- [11] TREACY M, EBBESEN T, GIBSON J. Exceptionally High Young's Modulus Observed for Individual Carbon Nanotubes [J]. *Nature*, 1996, 381: 678—680.
- [12] LEE C J, PARK J, KANG S Y, et al. Growth and Field Electron Emission of Vertically Aligned Multiwalled Carbon Nanotubes [J]. *Chemical Physics Letters*, 2000, 326: 175.
- [13] KHUN N W, TROCONIS B C R, FRANKEL G S. Effects of Carbon Nanotube Content on Adhesion Strength and Wear and Corrosion Resistance of Epoxy Composite Coatings on AA2024-T3 [J]. *Progress in Organic Coatings*, 2014, 77: 72—80.
- [14] JEON H, PARK J, SHON M. Corrosion Protection by Epoxy Coating Containing Multi-walled Carbon Nanotubes [J]. *Journal of Industrial and Engineering Chemistry*, 2013, 19: 849—853.
- [15] DOWLING A, CLIFT R, GROBERT N, et al. *Nanoscience and Nanotechnologies: Opportunities and Uncertainties* [R]. London: The Royal Society & The Royal Academy of Engineering Report, 2004: 61—64.
- (上接第35页)
- [13] ZHANG G A, CHENG Y F. Micro-electrochemical Characterization and Mott-Schottky Analysis of Corrosion of Welded X70 Pipeline Steel in Carbonate/Bicarbonate Solution [J]. *Electrochimica Acta*, 2009, 55(1): 316—324.
- [14] TANG X, CHENG Y F. Micro-electrochemical Characterization of the Effect of Applied Stress on Local Anodic Dissolution Behavior of Pipeline Steel under Near-neutral pH Condition [J]. *Electrochimica Acta*, 2009, 54(5): 1499—1505.
- [15] LIU Z Y, LI X G, DU C W, et al. Local Additional Potential for Effect of Strain Rate on SCC of Pipeline Steel in an Acidic Soil Solution [J]. *Corrosion Science*, 2009, 51: 2863—2871.
- [16] LIU Z Y, LI X G, CHENG Y F. Mechanistic Aspect of Near-neutral pH Stress Corrosion Cracking of Pipeline under Cathodic Polarization [J]. *Corrosion Science*, 2012, 55: 54—60.
- [17] LIU Z Y, LI X G, DU C W, et al. Stress Corrosion Cracking Behavior of X70 Pipe Steel in an Acidic Soil Environment [J]. *Corrosion Science*, 2008, 50: 2251—2257.
- [18] 王炳英, 霍立兴, 王东坡, 等. X80 管线钢在近中性 pH 溶液中的应力腐蚀开裂 [J]. *天津大学学报*, 2007, 40(6): 757—760.
- WANG Bing-ying, HUO Li-xing, WANG Dong-po, et al. Stress Corrosion Cracking of X80 Pipeline Steel in Near-neutral pH Value Solutions [J]. *Journal of Tianjin University*, 2007, 40(6): 757—760.
- [19] LIU Z Y, LIN L, HUANG Y H, et al. Mechanistic Aspect of Non-steady Electrochemical Characteristic during Stress Corrosion Cracking of an X70 Pipeline Steel in Simulated Underground Water [C]//2014, NACE International. [s. l.]: NACE, 2014.
- [20] 刘智勇, 王长朋, 杜翠薇, 等. 外加电位对 X80 管线钢在鹰潭土壤模拟溶液中应力腐蚀行为的影响 [J]. *金属学报*, 2011, 47(11): 1434—1439.
- LIU Zhi-yong, WANG Chang-peng, DU Cui-wei, et al. Effect of Applied Potential on Stress Corrosion Cracking of X80 Pipeline Steel in Simulated Yingtan Soil Solution [J]. *Acta Metallurgica Sinica*, 2011, 47(11): 1434—1439.